Scanning electrochemical microscopy of menadione-glutathione conjugate export from yeast cells

Janine Mauzeroll and Allen J. Bard*

Department of Chemistry and Biochemistry, University of Texas, 1 University Station, A5300, Austin, TX 78712

Contributed by Allen J. Bard, April 12, 2004

The uptake of menadione (2-methyl-1,4-naphthoquinone), which is toxic to yeast cells, and its expulsion as a glutathione complex were studied by scanning electrochemical microscopy. The progression of the *in vitro* reaction between menadione and glutathione was monitored electrochemically by cyclic voltammetry and correlated with the spectroscopic (UV–visible) behavior. By observing the scanning electrochemical microscope tip current of yeast cells suspended in a menadione-containing solution, the export of the conjugate from the cells with time could be measured. Similar experiments were performed on immobilized yeast cell aggregates stressed by a menadione solution. From the export of the menadione-glutathione conjugate detected at a 1-μm-diameter electrode situated 10 μm from the cells, a flux of about 30,000 thiodione molecules per second per cell was extracted. Numerical simulations based on an explicit finite difference method further revealed that the observation of a constant efflux of thiodione from the cells suggested the rate was limited by the uptake of menadione and that the efflux through the glutathione-conjugate pump was at least an order of magnitude faster.

To probe the transport activity of cells, we use scanning electrochemical microscopy (SECM), a technique that allows one to detect electroactive species at an ultramicroelectrode (UME) tip that can be positioned with high resolution. Here we monitor molecules that are transported from cells across membranes or ion channels into the external solution. A complete description of the fundamental principles, theoretical treatment, and applications of SECM has been published elsewhere (1). The transport rate for the detection of a detoxification product that is released from yeast cells, thiodione, when cells are stressed with menadione (2-methyl-1,4-naphthoquinone) was studied. This study relies on the direct electrochemical detection of thiodione and therefore differs from previously reported studies that relied on a double redox mediator system to study intracellular redox activity of yeast (2, 3).

Quinones are oxidants and electrophiles that are readily transported into cells, where they retain their ability to redox cycle, impose oxidative stress, and form covalent adducts with important cellular species. *In vivo*, quinone reduction to the semiquinone leads to the formation of reactive oxygen species (ROS) such as superoxide ion, peroxide, and hydroxyl radical. These are responsible for quinone-related oxidative damage associated with DNA cleavage and cell growth arrest (4). To cope with such stress, cells have enzymatic and nonenzymatic defenses. Glutathione (GSH; L-γ-glutamyl-L-cysteinylglycine), the major nonprotein sulfhydryl compound present in cells (5), plays a protective role in cells by means of its antioxidant properties by conjugation with harmful compounds and by chelation with heavy metals (6). With quinones, GSH detoxifies cells by undergoing nucleophilic addition to quinones to limit the irreversible modification of cellular macromolecules. The thioether conjugates (GS-X) can then be degraded to other substances (6) or actively removed from the intracellular media by using an ATP-dependent GS-X pump. For thiodione, the GS-X remains intact and is partly transported by the GS-X pump in the cell membrane (7, 8) into the extracellular medium, where it can be detected by SECM.

The export of GS-Xs from cells is ATP dependent and is mediated by an integral membrane glycoprotein belonging to the multidrug-resistance protein (MRP) family. There are six isoforms of this pump in humans, and numerous orthologs of it have been identified in other organisms, such as yeast (7). The universality of MRPs in different systems demonstrates the importance of these pumps in preventing the accumulation of GS-X in cells and in the final excretion of toxic compounds. Studying the effect of oxidative stress on the organism and export processes by these GS-X pumps is interesting because resistance to the cytotoxic action of drugs has been attributed to overexpression of both GSH *S*-transferases (GSTs) and the MRP proteins (9, 10).

When studying biological systems with SECM, one can choose between the feedback or generation collection (GC) modes. In general, the negative-feedback mode yields little information about the biological activity of the substrate and is mainly used to find the tip-to-substrate distance and image biological samples, as used recently with PC12 cells, dopamine-releasing immortal rat cells (11).

There have been a number of SECM studies of biological systems, such as enzymes and intact live cells. There was the study of photosynthesis on the leaves of *Tradescantia fluminensis* based on oxygen reduction profiles (12) and the study of resorption of osteoclasts on bone slices by using a Ca^{2+} potentiometric sensor (13). Since then, SECM has been extended to full cellular studies. Matsue and colleagues (14–18) reported live cell studies and monitored respiration rate changes by using oxygen reduction profiles for different cell types. In these experiments, oxygen is present in solution and is consumed by the living organism. More oxygen is consumed close to the cells, and a lower oxygen reduction current is measured. Mirkin and colleagues reported studies on human breast cells (19) and *Rhodobacter sphaeroides* (20), where the feedback mode of SECM was used to monitor the regeneration reaction of various mediators when exposed to cells. These studies provided useful information about the permeability of the membrane to a wide variety of redox couples and led to the development of a theoretical treatment that could extract kinetic information about these processes (21). SECM was reported to be able to distinguish between normal and malignant cells (22).

Materials and Methods

2-Methyl-3-glutathionyl-1,4-naphthoquinone Synthesis. 2-Methyl-3-glutathionyl-1,4-naphthoquinone (thiodione) was synthesized and recrystallized as previously reported (23), and was charac-

Abbreviations: GSH, glutathione; GS-X, GSH conjugate; GST, GSH *S*-transferase; SECM, scanning electrochemical microscopy; SMSE, standard mercury sulfate electrode; CV, cyclic voltammetry; UME, ultramicroelectrode.

*To whom correspondence should be addressed. E-mail: ajbard@mail.utexas.edu.

www.pnas.org/cgi/doi/10.1073/pnas.0402556101

terized by elemental analysis and H NMR (see *Supporting Materials and Methods*, which is published as supporting information on the PNAS web site).

Cell Growth and Sample Preparation. *Saccharomyces cerevisiae* cells (strain day4, day4vac) were grown on rich medium plates [10 g of yeast extract (Fischer), 20 g of peptone (Fluka), 20 g of dextrose (Fluka) filtered after autoclaving, 20 g of agar (Fluka), and 1 pellet of NaOH in 1 liter of water] in an incubator at 37.5°C for 3 days.

To carry out the bulk yeast cell experiments, $\approx 10^9$ cells were transferred to an electrochemical cell containing degassed 0.5 mM menadione. This yeast concentration in a stock solution was determined from successive dilution measurements on agar plates. To determine the concentration of living cells that contributed to the electrochemical signal, a 50-μl aliquot of this solution was diluted with 10 ml of PBS. This dilution procedure was repeated three additional times, so that the final solution was 1.6×10^9 times more dilute than the stock solution. Rich media plates were made and then plated with 200-μl aliquots of the different diluted solutions. Three sets of five plates were incubated for 3 days at 37.5°C and the number of colonies produced was counted. Only the plates with large numbers of isolated, well-separated colonies that did not show any signs of discoloration were used for the concentration determination. Because a colony is produced from a single cell, the original concentration of cells in the solution used in the electrochemical experiments could be estimated. On average, 10^9 living cells contributed to the electrochemical current measured in the bulk cell experiments. Turbidity measurements were not used to determine concentrations because they are based on scattering from the cell walls and do not differentiate between living and dead cells. Because a large number of cells produce a relatively small oxidation current, experiments with immobilized cell aggregates have to be carried out with small solution volumes to be able to detect the thiodione export.

To attach the yeast cells to glass, the glass surface was cleaned overnight in 1% HCl/70% ethanol/29% water (by volume) and then rinsed with water. The glass slides were dried in an oven at 110°C, whereas the glass-bottom Petri dishes (Delta T dishes, Bioptechs, Butler, PA) were air dried. The glass surfaces were coated with a 10% poly(L-lysine) (Sigma) solution for 5 min, after which they were thoroughly rinsed and dried in the oven at 60°C for 1 h. Yeast cells were then transferred to the phosphate buffer, stirred, and poured over the poly(L-lysine)-treated glass Petri dish or slides. The cell solution contacted the treated glass for 20 min and was drained, followed by rinsing and drying. Fluorescence cytotoxicity experiments with 10 mM FUN1 fluorescent dye (Molecular Probes) incubated 1 h in the dark confirmed that the immobilized cells were alive for several hours. Description of electrode fabrication can be found in *Supporting Materials and Methods*.

Electrochemistry. A CHI model 900 scanning electrochemical microscope (CH Instruments, Austin, TX) was used to control the tip potentials, obtain the approach curves, and monitor the tip-to-substrate distance.

The electrochemical behavior of synthesized thiodione, the spontaneous reaction between menadione and GSH, and the bulk yeast cell experiment were monitored by cyclic voltammetry (CV) and used both 1- to 4- and 25-μm Pt electrodes. The particular experimental parameters are given in the figure legends. The course of the *in vitro* reaction and the absorbance of the synthesized compound were confirmed by UV–visible spectroscopy (Milton-Roy Spectronic 3000 array).

To perform the experiments on the immobilized yeast cell aggregates, the SECM head was placed on the stage of an inverted microscope (Eclipse TE300 Nikon Inverted Microscope, Melville, NY) to facilitate tip positioning over the cells (Fig. 1). The tip was first positioned in air over the yeast aggregates by using the piezoelectric drivers of the SECM. The quartz tips are very flexible and do not break upon contact with the glass surface. The electrode was therefore positioned in air until the tip was visually seen to touch a bare glass region. The tip was then retracted 10 μm away from the sample and positioned over an aggregate optically. The tip and fiber optic were held in the middle of a Ag/AgCl reference coil so that a 50-μl drop of menadione solution could be supported and would just contact the sample surface. These experiments were performed in a two-electrode setup because the currents are small with the UMEs used. The fiber optic was used to illuminate the sample and reduce the shadowing effect of the tip holder. Once positioned, a small drop of buffer was placed in the reference coil and a voltammogram was recorded. The drop was then aspirated out and replaced by a 50-μl drop of degassed menadione (0.1 mM) and CV was started immediately.

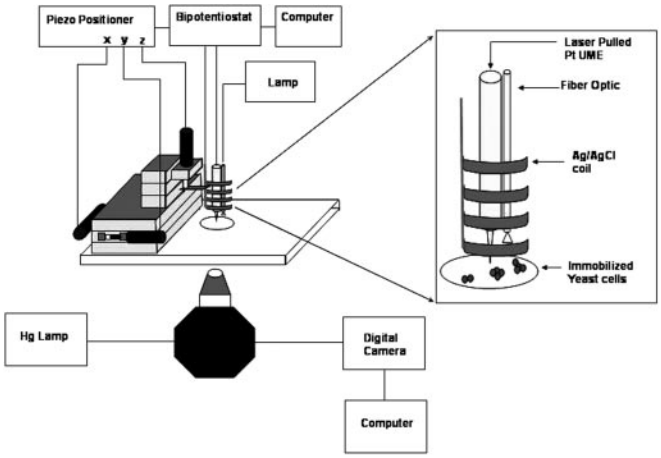

Fig. 1. Experimental setup for the electrochemical detection of the export of thiodione from immobilized yeast aggregates by using laser-pulled Pt UMEs.

Results and Discussion

Thiodione Electrochemistry. The voltammograms of solutions containing menadione, GSH, and synthesized thiodione are shown in Fig. 2*A*. The GSH does not show any redox reactions at Pt under these conditions, whereas the menadione and thiodione both show a two-electron reduction of the quinone moiety at about −0.7 V vs. a SMSE. The steady-state current for thiodione is significantly smaller than that of the menadione at the same concentration because thiodione is larger and has a smaller diffusion coefficient, 4.0×10^{-6} cm^2·s^{-1}, vs. 8.0×10^{-6} cm^2·s^{-1} for menadione as determined from the limiting currents of the reduction waves. The thiodione reduction $E_{1/2}$ is about 150 mV more negative than that of menadione. This spacing is insufficient for clear differentiation between the two compounds by using CV. These results agree with previous studies that reported similar decreases in $E_{1/2}$ for thiodione versus menadione as measured by HPLC with electrochemical detection (24).

The thiodione conjugate can be distinguished from menadione by its irreversible oxidation wave at about 0.1 V vs. SMSE (Fig. 2*B*), where neither menadione nor GSH gives any electrochemical response. This allows one to analyze simultaneously for the conjugate and the combined menadione and thiodione by CV during the spontaneous reaction of menadione and GSH by the nucleophilic addition of the glutathionyl at the 3 position of the menadione ring. Upon mixing equimolar amounts of menadione and reduced GSH, the oxidation wave is seen to increase

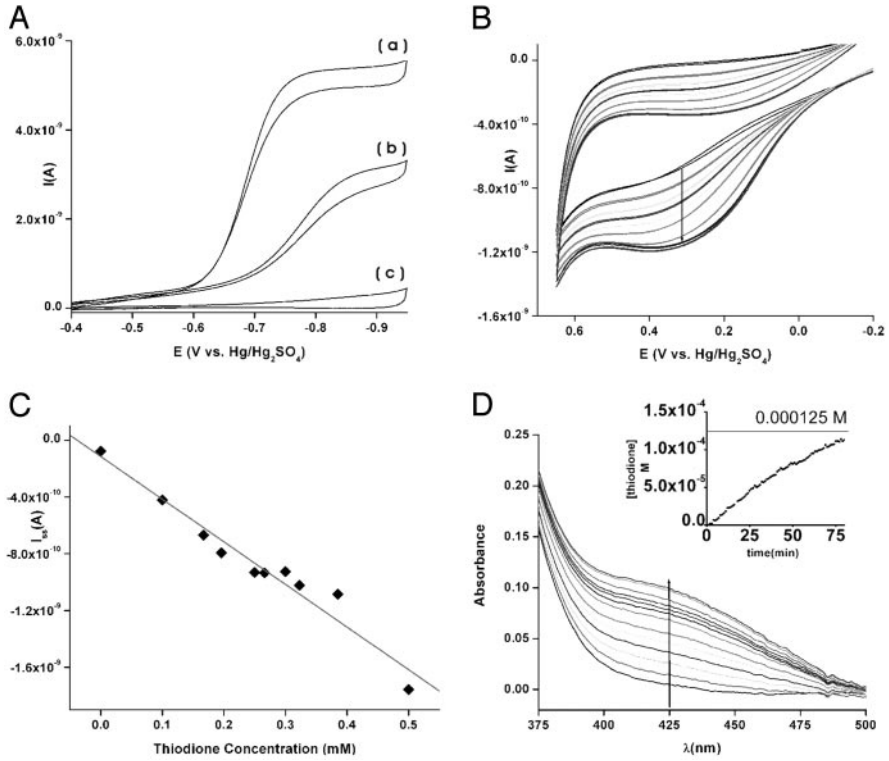

Fig. 2. (*A*) Voltammetric response of 0.5 mM menadione (traces a), 0.5 mM synthesized thiodione (traces b), and 0.5 mM GSH (traces c). (*B*) Oxidation wave for the formation of thiodione with time. Equimolar amounts of menadione (0.25 mM) and GSH (0.25 mM) spontaneously react to form thiodione. The limiting current of the oxidation wave becomes larger with time until the reaction is complete. Only a small set of nonsequential CV traces are presented. (*C*) Calibration curve for the synthesized thiodione; oxidation current vs. concentration of thiodione. The responses in *A*–*C* were obtained in PBS at pH 7, the potential was measured with respect to a standard mercury sulfate electrode (SMSE), and the Pt tip diameter was 25 μm. A scan rate of 50 mV/s was used in the experiments. Argon was bubbled through all solutions for 30 min and a 0.5-mm Pt auxiliary electrode was used. (*D*) Appearance of a broad shoulder at 425 nm during thiodione formation. Equimolar amounts of menadione (0.125 mM) and GSH (0.125 mM) in PBS pH 7 electrolyte spontaneously reacted to form thiodione. As thiodione is formed, the absorbance at 425 nm increases. (*Inset*) The calculated increase in concentration of thiodione with time.

with time until it levels off to a limiting value upon completion. The synthesized compound was used to show that the limiting current was proportional to the concentration (Fig. 2*C*).

The mechanism of the electrochemical oxidation of thiodione has yet to be elucidated but is probably an irreversible oxidation of the sulfide to the sulfoxide, based on previous reports of the electrochemistry of similar sulfur-containing compounds (25). From H NMR data (both in water and in dimethyl sulfoxide), the electrochemistry at large electrodes (data not shown) and previously reported studies (26), the menadione-glutathione conjugate probably remains in the oxidized form after the conjugation reaction.

The formation of thiodione was also monitored by UV–visible spectrophotometry of the solution at various times during the conjugation reaction and confirms the reported growth of a broad shoulder at 425 nm (Fig. 2*D*) (27). The concentration of thiodione increased with time until completion, and the final concentration observed was very close to 0.125 mM, the expected yield calculated from the initial concentrations (Fig. 2*D Inset*). The reaction between dissolved menadione and GSH is slow, with a half-life of the reaction, $t_{1/2}$, of 36 min. This long reaction time supports the idea that in cells, the conjugation is enzyme assisted, consistent with studies showing that GSTs catalyze the formation of GS-X in *S. cerevisiae* (28, 29).

Bulk Yeast Cell Experiments. About 10^9 cells in 2 ml of 0.5 mM menadione solution were used to detect the export of thiodione from yeast cells. Menadione readily diffuses into the cells, where it conjugates with intracellular GSH and, by means of the yeast ortholog of the multidrug-resistance protein pump, is either exported into the extracellular medium or sequestered in a vacuole (6, 29–32). Export of thiodione to the extracellular medium was monitored with a 25-μm Pt electrode immersed in the solution, where the voltammogram shows the growth of the anodic thiodione wave with time at the same potential as that seen in the thiodione synthesis experiment (Fig. 3 *A* and *B*). This observation confirms the electrochemical detection of the conjugate exported from yeast cells as a result of menadione-imposed oxidative stress.

To examine immobilized cells, as discussed in the next section, a smaller (4-μm) tip is required. To understand better the sensitivity of such a tip, similar bulk cell experiments (not shown) and the *in vitro* reaction of menadione and GSH were also carried out with smaller, 4-μm, tips. As seen in Fig. 3*C*, the limiting current obtained upon completion of the reaction is almost identical to that calculated from the initial concentrations of reagents. To obtain good quantitative results with the small UME, the solution had to be degassed and a large potential sweep was required. The large potential sweep was useful in desorbing material from the electrode surface and ensured good quantitative results.

Studies have suggested that GSH itself might be released from cells by the ATP-dependent low-affinity transport YCF1 transporter (30). The amounts of extracellular GSH, used as a signaling molecule, in that report was 0.2% of the intracellular concentration of GSH, normally between 1 and 10 mM. Any appreciable amounts of GSH exported during our measurements would, in time, compromise the response observed because of its

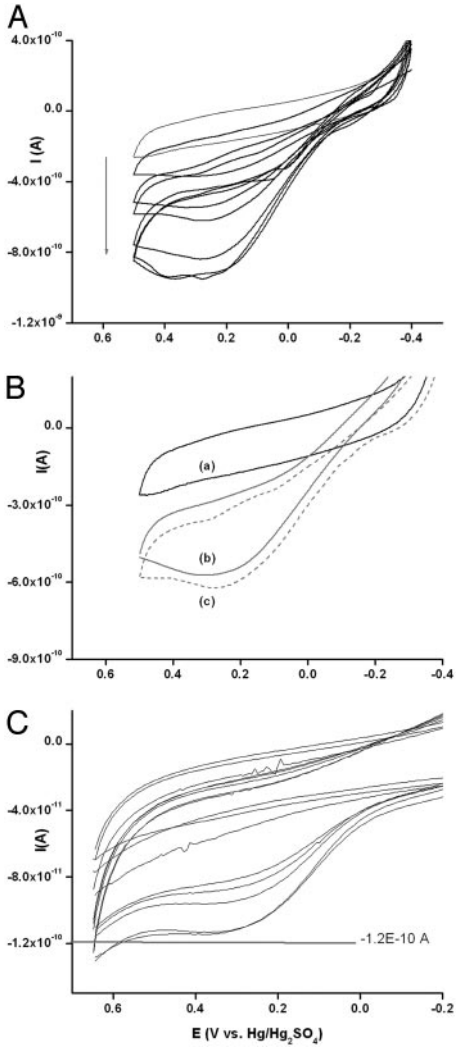

Fig. 3. (*A*) Electrochemical detection of thiodione exported from bulk DAY4 yeast cells at a 25-μm Pt electrode. About 10^9 cells were treated with 0.5 mM menadione in PBS pH 7 electrolyte. The potential was cycled between −0.95 and 0.5 V at 10 mV/s. The wave height increased with time until it reached a steady-state value. (*B*) Comparison of the oxidation response at a 25-μm Pt electrode for PBS pH 7 buffer (traces a) to response of the synthesized thiodione (traces b) and that recorded from the bulk DAY4 yeast cells (traces c). (*C*) Electrochemical detection of the formation of thiodione at a 4-μm Pt UME from the spontaneous reaction of menadione (0.25 mM) and GSH (0.25 mM) in PBS pH 7.4 solution. The horizontal line represents the expected steady-state current value for 100% completion of the reaction. The potential was cycled between −0.95 and 0.5 V at 50 mV/s. All potentials were measured with respect to SMSE, and a 0.5-mm Pt auxiliary electrode was used. All solutions were degassed with argon for 30 min.

reaction with extracellular menadione. Using a hanging mercury drop electrode (HMDE) and mercury hemispherical electrodes (33), we repeated the bulk yeast cell experiments in the absence of extracellular menadione. GSH alone in a PBS solution gives a well defined quasireversible oxidation signal at low concentrations at Hg (see Fig. 7, which is published as supporting information on the PNAS web site). At higher concentrations, adsorption processes dominate and alter the response (34). In the presence of bulk cells neither the HMDE nor the hemispherical mercury UMEs detected any significant amount of GSH coming from the cell over a time period of hours. This lack of detection was not due to electrode fouling, because at the end of these experiments an aliquot of GSH at a concentration of 0.5 mM was added and a good electrochemical response was observed. Thus, if there is any GSH exported along with the thiodione, the amounts are sufficiently small that they do not significantly affect the detection of the export of the conjugate.

Immobilized Yeast Cell Aggregate Experiment. Under physiological conditions, *S. cerevisiae* cells have a negatively charged cell surface (35), where surface macromolecules, such as mannoproteins and glucan that contain phosphodiester, amino, and carboxyl groups, produce charge on the cell that aids in adhesion processes (36). Yeast cells can therefore be immobilized on glass supports that have been pretreated with poly(L-lysine). The immobilized cells remain alive for several hours, as confirmed by fluorescence studies performed with FUN1 viability dye (Fig. 4 *A* and *B*), which identified the appropriate dose of menadione (100 μM) to be used and documented the effect of the microscope Hg lamp exposure on the cell viability (data not shown).

The concentration of the thiodione exported from 131 cells is presented in Fig. 4*E*. At 0.35 V vs. SMSE, the thiodione signal increases with time. Fig. 4*C* shows an optical micrograph of the 4-μm tip positioned 10 μm above the yeast cell aggregate made during an SECM scan. Cyclic voltammograms were taken with time after introduction of the menadione (Fig. 5). The current at 0.35 V was measured and converted to thiodione concentration by using the steady-state current expression for a disk UME. The steady-state tip current, I_{ss}, given by

$$I_{ss} = 4nFDC_o a, \qquad [1]$$

where the number of electrons is 2, F is the Faraday constant, D is the diffusion coefficient of thiodione in solution (4×10^{-6} $cm^{-2}{\cdot}s^{-1}$), C_o is the concentration of thiodione, and a is the radius of the Pt electrode (2 μm). The response was background subtracted for the electrolyte signal. The first CV showed a response identical to that of the background and so the first run was assigned as $t = 0$ s.

The general shape of conjugate export in Fig. 4*E* is consistent with that observed in other studies that looked at efflux of thiodione from rat platelet-rich plasma by using a HPLC–UV–visible detection scheme (37) and that of the electrochemical detection of doxorubicin export from Chinese hamster ovary cells (38).

Model of Thiodione Release. A simplified model (Fig. 4*D*) was used to calculate the thiodione efflux per cell per second, J_{cell}. Menadione, M_o, readily diffuses into the yeast cells with a heterogeneous rate constant, k_{in}. Inside the cell, the menadione (M_i) is conjugated (homogeneous rate constant, k_{con}) by GSH (G) and is converted to thiodione (MG_i) by the action of GSTs (28). This conjugation is known to be fast relative to the uptake of menadione and the efflux of thiodione, based on reported rat hepatocyte studies. Inside the cell, the formation of the conjugate is rapid as opposed to the slower *in vitro* reaction between menadione and GSH (39). Platelet-rich plasma studies in rats also showed that as much menadione is consumed by conjugation as is taken up by the cells based on HPLC with absorbance measurements (37). Once conjugated, thiodione is rapidly exported into the extracellular medium (MG_o) with a heterogeneous rate constant, k_{out}, by the GS-X pump.

For a substrate such as the aggregate of yeast cells that is large compared with the tip diameter, one can assume linear diffusion of MG_o leaving the cell. We assume that the flux of MG_o ($mol{\cdot}s^{-1}{\cdot}cm^{-2}$), J, is constant, with an initial concentration of thiodione of zero and the distance $x = 0$ taken as the cell surface. The concentration profile of thiodione for this constant flux boundary condition at the substrate can be obtained from the equivalent expression for a constant current process at an electrode (with $J = i/nFA$) (ref. 40, equation 8.2.11)

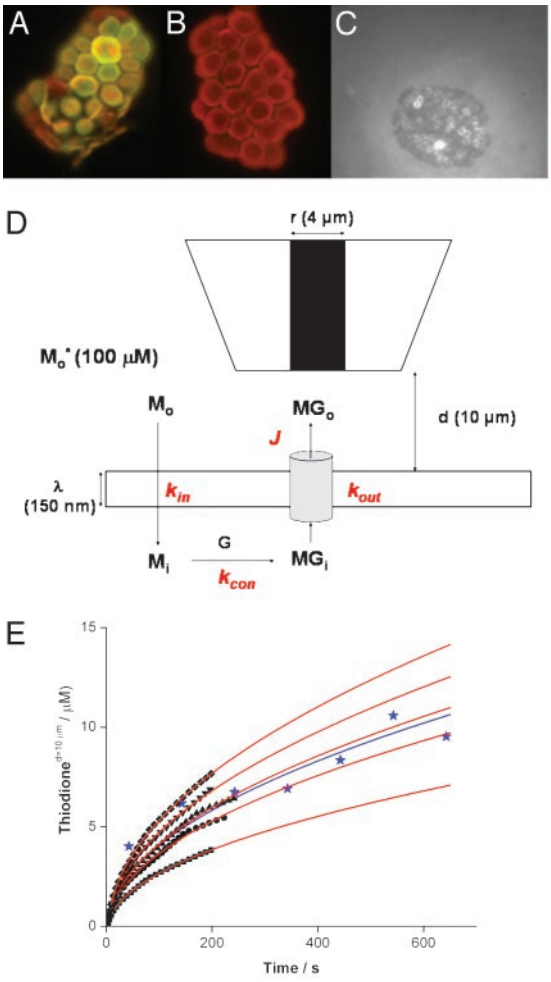

Fig. 4. (*A*) Positive control of living immobilized DAY4 yeast cells on glass. The cells were incubated with 10 mM FUN1 dye for 1 h. The living cells metabolize the dye to produce diffuse green fluorescence in the cytosol and red cylindrical features. (*B*) Negative control of living immobilized DAY4 yeast cells on glass. The immobilized cells were incubated in the UV reactor for 1 h. The dead cells do not metabolize the dye and produce diffuse red fluorescence with no features. (*C*) Optical micrograph of the 4-μm Pt wire from the tip (bright spot) over the immobilized aggregate of cells before the start of the collection experiment. The tip was 10 μm away from the glass surface. (*D*) Representation of the theoretical model used to treat the immobilized aggregate collection experiments. The outside menadione (M_o) diffuses through the cell wall and membrane with time with a rate constant, k_{in}. Once inside, the menadione (M_i) rapidly conjugates with intracellular GSH (k_{con}). The intracellular thiodione (MG_i) is then pumped out of the cell by the GS-X analog pump with a rate constant, k_{out}. The expelled thiodione (MG_o) is then detected at the UME with time. The proposed model assumes a constant flux, J, of thiodione from the yeast. (*E*) Plot of experimental thiodione concentration released from an aggregate of 131 cells with time (⋆). Fit of experimental concentrations to Eq. **2** for $x = 10$ μm; $D = 4 \times 10^{-6}$ cm^2·s^{-1} (blue line). Numerical simulation results for $k_{in} = 5 \times 10^{-6}$ cm/s (■), $k_{in} = 7 \times 10^{-6}$ cm/s (●), $k_{in} = 8 \times 10^{-6}$ cm/s (▲), $k_{in} = 9 \times 10^{-6}$ cm/s (▼), $k_{in} = 1 \times 10^{-5}$ cm/s (◆). All numerical simulations were solved with $k_{out} = 1 \times 10^{-4}$ cm/s and $k_{con} = 1$ s^{-1}. Fit of individual numerical simulation to Eq. **2** with $x = 10$ μm; $D = 4 \times 10^{-6}$ cm^2·s^{-1} (red line).

$$C(x, t) = \frac{2J}{D}\left[\left(\frac{Dt}{\pi}\right)^{1/2} \exp(-x^2/4Dt) - \frac{x}{2}\,\mathrm{erfc}\{x/2(Dt)^{1/2}\}\right], \quad [2]$$

where D (cm^2·s^{-1}) is the diffusion coefficient of thiodione in solution, x (cm) is the distance from the cell, and t (s) is time. A

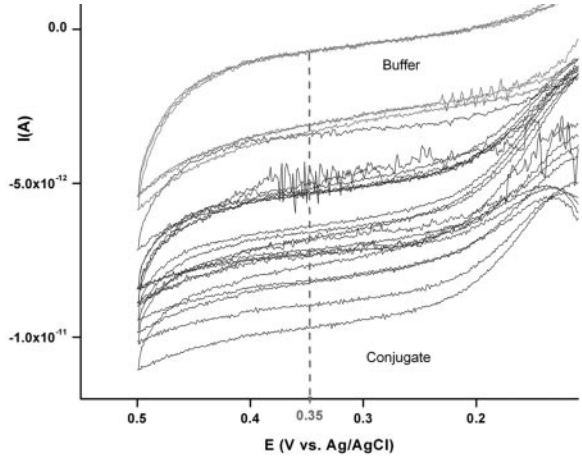

Fig. 5. Collection of exported thiodione from the immobilized aggregate of DAY4 yeast cells after the imposition of oxidative stress by 50 μl of 0.1 mM menadione. The response was collected between −0.5 and 0.5 V at a 20 mV/s. The potential was recorded with respect to an Ag/AgCl electrode coil in a two-electrode configuration using a 4-μm Pt UME.

similar approach was previously used in a study of the efflux of doxorubicin from an auxotrophic mutant of Chinese hamster ovary cells, AUXB1, and its multidrug-resistant strain (41). The concentration at the tip is obtained by setting x equal to the distance between tip and cell. The yeast experimental data in Fig. 4*E* were fit to Eq. **2** by using MATHEMATICA (NonLinear Regression package, Wolfram Research, Champaign, IL). The nonlinear curve fit gave a $J = 7.5 \times 10^{-13}$ mol·s^{-1}·cm^{-2} [confidence interval, (6.7 to 8.4) $\times 10^{-13}$ mol·s^{-1}·cm^{-2}].

The thiodione detected by the UME originated from an aggregate of cells that was isolated from other single cells or aggregates (Fig. 4*C*). This particular yeast aggregate contained 131 cells, each with an average 3-μm diameter, and was larger than the 4-μm Pt tip, so that linear diffusion of thiodione from the aggregate can be assumed. The flux per cell per unit time, J_{cell} (5.33×10^{-20} mol/s per cell), was obtained by multiplying the flux, J, by the area of the aggregate, A_{agg} (9.28×10^{-6} cm^2), divided by the number of yeast cells in the aggregate. This value is in general agreement with the previous study (41), although a direct comparison to their J values is not possible because of the large difference between the cell lines as well as the assumption that the tip electrode was at $x = 0$ (made to simplify the fitting).

The concentration of thiodione (≈10 μM) expelled from the cell represents only 10% of the concentration of menadione (≈100 μM) used to stress the cells. The vacuolar sequestration of thiodione is thus probably an important detoxification pathway. Vacuolar sequestration and cellular extrusion of GSH-conjugated xenobiotics and catabolites by GS-X pumps is an important detoxification mechanism in many organisms (42). The confinement of conjugated compounds, heavy metals, and catabolites in plants (43) and in yeast (29, 31) is well known. In *S. cerevisiae*, vacuolar sequestration of many GSH conjugates is partly accomplished by a GS-X pump imbedded in the vacuolar membrane (30, 31, 38, 44, 45). This pump is also present in the cytosolic membrane and transports the thiodione into the extracellular medium, where it can be detected by SECM. Bulk experiments with vacuole-deficient DAY4 (46) mutants were attempted to see whether increased export could be observed. In these experiments, thiodione export was observed (data not shown) but aggregate experiments were not successful because the small size of these mutants compared with the wild-type strain.

The above model assumes that the probe electrode does not significantly disturb the thiodione concentration profile. This is a reasonable assumption because the probe electrode is small. Moreover, numerical simulations (to be reported elsewhere) of the concentration profiles above a surface with a constant flux of product, with and without a tip, were essentially the same. We also assume that diffusion controls mass transfer between the cells and the tip with negligible perturbation because of natural convection that often occurs in measurements extending beyond about 100 s. However, if only the first three points are used to fit Eq. **2**, a $k_{in} = 1 \times 10^{-5}$ cm/s is obtained. This value is only 20% larger than k_{in} found by using the entire curve (within experimental error) and suggests that convection does not appreciably perturb the longer time measurements, as also assumed in earlier studies (41). The simulation also gives quantitative results that are essentially the same as those of Eq. **2**. In the simulations, a constant-flux condition was attained only when the rate of uptake of menadione was an order of magnitude lower than the efflux rate and the homogenous conjugation of menadione to GSH was fast. The rate of uptake of menadione extracted from the numerical simulations is $k_{in} = 8 \times 10^{-6}$ cm/s. Based on the numerical simulations, the rate of efflux of thiodione by the GS-X pump must be at least an order of magnitude higher than the rate of uptake for a constant flux boundary condition to exist. Under these conditions a value for k_{out} cannot be obtained. The outcome of this theoretical treatment suggests that menadione slowly diffuses into the cell and is followed by fast conjugation with GSH to produce thiodione that is rapidly pumped out of the cell.

That the uptake of menadione is the slow step is not surprising when one considers that the uptake requires passive diffusion across the membrane, whereas the export of thiodione is assisted by the GS-X pump. We have carried out similar measurements on a mammalian cell that shows less hindered transport across the membrane. Moreover, these larger cells (20–45 μm in diameter) allow SECM imaging of the export process with a single cell. These results will be reported elsewhere.

Conclusions

Thiodione can be identified and detected electrochemically in solution during the reaction of menadione and GSH. The electrochemical detection of thiodione was corroborated by UV–visible studies. It can also be detected when exported from a bulk yeast cell suspension and from small yeast cell aggregates on a surface exposed to menadione. From the efflux of thiodione from an isolated yeast cell aggregate, a flux, J_{cell}, of 5.3×10^{-20} mol per cell per second (or about 30,000 molecules per cell per second) was found, and suggests that the rate of uptake of menadione by the yeast cells (with a rate constant of $k_{in} = 8 \times 10^{-6}$ cm/s) is the rate-determining process. The rate of efflux of thiodione through the GS-X pump is at least an order of magnitude higher than the latter for the constant-flux condition to obtain.

The yeast cells DAY4 and DAY4vac were graciously donated by Prof. D. Appling of the Chemistry and Biochemistry Department (University of Texas). We appreciate the help and advice of Dr. S. Chang. We are indebted to Dr. José L. Fernández for his help with the numerical simulations. We thank Dr. Bob LeSeur and Dr. Steen B. Schougaard for their help with the MATHEMATICA software. This work was funded by the Edward G. Weston Summer Research Fellowship of the Electrochemical Society and by the National Science Foundation (CHE 0109587) (University of Texas).

1. Bard, A. J. & Mirkin, M. V., eds. (2001) *Scanning Electrochemical Microscopy* (Dekker, New York).
2. Rabinowitz, J. D., Vacchino, J. F., Beeson, C. & McConnell, H. M. (1998) *J. Am. Chem. Soc.* **120,** 2464–2473.
3. Heiskanen, A., Yakovleva, J., Spégel, C., Taboryski, R., Koudelka-Hep, M., Emncus, J. & Ruzgas, T. (2004) *Electrochem. Commun.* **6,** 219–224.
4. Monks, T. J. & Lau, S. S. (1998) *Annu. Rev. Pharmacol. Toxicol.* **38,** 229–255.
5. Reed, D. J. & Meredith, M. J. (1985) in *Bioactivation of Foreign Compounds*, ed. Anders, M. W. (Academic, Orlando, FL), pp. 71–108.
6. Foyer, C. H., Theodoulou, F. L. & Delrot, S. (2001) *Trends Plant Sci.* **6,** 486–492.
7. Keppler, D. (1999) *Free Radical Biol. Med.* **27,** 985–991.
8. Sies, H. (1999) *Free Radical. Biol. Med.* **27,** 916–921.
9. Morrow, C. S., Smitherman, P. D. & Townsend, A. J. (1998) *Biochem. Pharmacol.* **56,** 1013–1021.
10. Morrow, C. S., Smitherman, P. K., Diah, S. K., Schneider, E. & Townsend, A. J. (1998) *J. Biol. Chem.* **273,** 20114–20120.
11. Liebetrau, J. M., Miller, H. M., Baur, J. E., Takacs, S. A., Anupunpisit, V., Garris, P. A. & Wipf, D. O. (2003) *Anal. Chem.* **75,** 563–571.
12. Tsionsky, M., Cardon, Z. G., Bard, A. J. & Jackson, R. B. (1997) *Plant Physiol.* **113,** 895–901.
13. Berger, C. E. M., Rathod, H., Gillespie, J. I., Horrocks, B. R. & Datta, H. (2001) *J. Bone Miner. Res.* **16,** 2092–2102.
14. Yasukawa, T., Kaya, T. & Matsue, T. (1999) *Anal. Chem.* **71,** 4637–4641.
15. Nishizawa, M., Takoh, K. & Matsue, T. (2002) *Langmuir* **18,** 3645–3649.
16. Takii, Y., Takoh, K., Nishizawa, M. & Matsue, T. (2003) *Electrochim. Acta* **48,** 3381–3385.
17. Kaya, T., Nishizawa, M., Yasukawa, T., Nishiguchi, M., Onouchi, T. & Matsue, T. (2001) *Biotechnol. Bioeng.* **76,** 391–394.
18. Shiku, H., Shiraishi, T., Ohya, H., Matsue, T., Abe, H., Hoshi, H. & Kobayashi, M. (2001) *Anal. Chem.* **73,** 3751–3758.
19. Liu, B., Rotenberg, S. A. & Mirkin, M. V. (2000) *Proc. Natl. Acad. Sci. USA* **97,** 9855–9860.
20. Cai, C., Liu, B., Mirkin, M. V., Frank, H. A. & Rusling, J. F. (2002) *Anal. Chem.* **74,** 114–119.
21. Biao, L., Rotenberg, S. A. & Mirkin, M. V. (2002) *Anal. Chem.* **74,** 6340–6348.
22. Feng, W., Rotenberg, S. A. & Mirkin, M. V. (2003) *Anal. Chem.* **75,** 4148–4154.
23. Nickerson, W. J., Falcone, G. & Strauss, G. (1963) *Biochemistry* **13,** 537–543.
24. Buffinton, G. D., Öllinger, K., Brunmark, A. & Cadenas, E. (1989) *Biochem. J.* **257,** 561–571.
25. Chambers, J. Q. (1978) in *Encyclopedia of Electrochemistry of the Elements, XII*, eds., Bard, A. J. & Lund, H. (Dekker, New York), Vol. 12, p. 453.
26. Lau, S. S., Jones, T. W., Highet, R. J., Hill, B. A. & Monks, T. J. (1990) *Toxicol Appl. Pharmacol.* **104,** 334–350.
27. Zadzinski, R., Fortuniak, A., Bilinski, T., Grey, M. & Bartosz, G. (1998) *Biochem. Mol. Biol. Int.* **44,** 747–759.
28. Sies, H. & Ketterer, B., eds. (1988) *Glutathione Conjugation: Mechanisms and Biological Significance* (Academic, London).
29. Penninckx, M. (2000) *Enzyme Microb. Technol.* **26,** 737–742.
30. Rebbeor, J. F., Connolly, G. C., Dumont, M. E. & Ballatori, N. (1998) *J. Biol. Chem.* **273,** 33449–33454.
31. Li, Z.-S., Szczypka, M., Lu, Y. P., Thiele, D. J. & Rea, P. A. (1996) *J. Biol. Chem.* **271,** 6509–6517.
32. Falcón-Pérez, J. M., Mazón, M. J., Molano, J. & Eraso, P. (1999) *J. Biol. Chem.* **274,** 23584–23590.
33. Mauzeroll, J., Hueske, E. A. & Bard, A. J. (2003) *Anal. Chem.* **75,** 3880–3889.
34. Jin, W., Zhao, X. & Xia, L. (2000) *Electroanalysis* **12,** 858–862.
35. Ahimou, F., Denis, F. A., Touhami, A. & Dufrêne, Y. F. (2002) *Langmuir* **18,** 9937–9941.
36. Eddy, A. A. & Rudin, A. D. (1958) *Proc. R. Soc. London Ser. B* **148,** 419–432.
37. Chung, J.-H., Seo, D.-C., Chung, S.-H., Lee, J.-Y. & Seung, S.-A. (1997) *Toxicol. Appl. Pharmacol.* **142,** 378–385.
38. Lu, H. & Gratzl, M. (1999) *Anal. Chem.* **71,** 2821–2830.
39. Di Monte, D., Ross, D., Bellomo, G., Eklöw, L. & Orrenius, S. (1984) *Arch. Biochem. Biophys.* **235,** 334–342.
40. Bard, A. J. & Faulkner, L. R. (2001) *Electrochemical Methods* (Wiley, New York), 2nd Ed., p. 309.
41. Yi, C. & Gratzl, M. (1998) *Biophys. J.* **75,** 2255–2261.
42. Klein, M., Mamnun, Y. M., Eggmann, T., Schüller, C., Wolfger, H., Martinoia, E. & Kuchler, K. (2002) *FEBS* Lett. **520,** 63–67.
43. Martinoia, E., Klein, M., Geisler, M., Bovet, L., Forestier, C. & Kolukisaoglu, Ü., Müller-Röber, B. & Schulz, B. (2002) *Planta* **214,** 345–355.
44. Szczypka, M. S., Wemmie, J. A., Moye-Rowlet, W. S. & Thiele, D. J. (1994) *J. Biol. Chem.* **269,** 22853–22857.
45. Tommasini, R., Evers, R., Vogt, E., Mornet, C., Zaman, G. J., Schinkel, A. H., Borst, P. & Martinoia, E. (1996) *Proc. Natl. Acad. Sci. USA* **93,** 6743–6748.
46. Chan, S. Y. & Appling, D. R. (2003) *J. Biol. Chem.* **278,** 43051–43059.